Study on the Visco-Elastic Deformation of Deposited Snow

Kenji SHINOJIMA
篠 島 健 二
Disaster Prevention Laboratory, Railway Technical Research Institute
Japanese National Railways, Sapporo, Japan

Abstract

Columnar snow samples (20 cm in length, 20 cm^2 in sectional area) cut out from horizontally deposited snow were tested on two types of deformation. In the first test, the deformation of uniaxial compression, elongation or torsion under constant load was investigated and in the second, the same points under constant various speeds were investigated.

It was assumed that the test results would be influenced by the following experimental factors, *i.e.*, the snow type, the density and the temperature of the snow sample, the test period, the deformation speed and the preservation time of snow specimen in the cold room, etc.

a) In various deformation tests under static load, the loading time was divided into two types (short duration test: 30 minutes for compression and elongation and 60 minutes for torsion; long duration test: about 60 hours in all cases) for compression.

The strain-time relations observed in the short duration test were analyzed particularly by means of the creep-equation derived theoretically from a dynamical model consisting of a serial combination of a Maxwell's element and a Voigt's element. Coefficients of visco-elasticity and Poisson's ratio were calculated from the creep curves and the strain-time relations respectively and their respective correlations were discussed theoretically. Over all test temperatures ranged from 0 to −37°C.

b) In various deformation tests under constant speed, the stress-time relations obtained could be analyzed by the aid of Boltzmann's fundamental equation. It was assumed that the behaviors of stress in the sample caused by the various deformations (compressive, tensile and torsional deformations) were influenced by the following conditions: the snow type, the density and the temperature of the snow sample, the velocity and the period of deformation, etc. Test temperature ranged from −12 to −26°C; velocities of deformation ranged from 0.1 to 0.5 mm/min in compression and tension and from 0.56 to 2.25°/min in torsion.

I. Introduction

A snow cover is subjected to various deformations and sometimes breakes down by internal stresses created by its own weight or by external forces. In order to investigate the problems of snow pressure etc., it is generally required to obtain the relations between the three fundamental stresses, *i.e.*, compressive, tensile and shearing stresses and the deformation corresponding to each of them in relation to the snow temperature.

Deposited snow has been generally considered as a kind of visco-elastic material characterized phenomenally by the properties of creep, relaxation, fluidity and strength, etc. and may be regarded as a homogeneous material on a stratification, accumulated by a continuous precipitation. However, strictly speaking, it is a three dimensional network-structure consisting of a number of small ice particles and subjected to a continuous internal metamorphism.

However, in the present work, experimental methods of creep and relaxation were adopted in order to find the characteristics of visco-elasticity in the snow provided that the density is small. As stated above, snow continuously undergoes certain physical changes and their respective rates are effected by the snow temperature and forces acting on the snow sample. Accordingly, the test periods were divided into comparatively short and long durations.

II. Snow Specimens

Cubic masses of snow were taken from the horizontal fields at Shiozawa (Winter 1961～'62, Winter 1962～'63), Niigata prefecture and at Sapporo (Winter 1963～'64), Hokkaido in Japan, and were preserved in the cold room during the experimental period. Snow samples used for each test were cut out from these cubic masses with a cylindrical acrylite sampler having a cross-sectional area of 20 cm^2 and a length of 20 cm. These were set on each apparatus after weighing. After cooling to certain test temperature, each test was undertaken.

III. Experimental Instruments and Methods

1) INSTRUMENTS OF DEFORMATION TESTS UNDER VARIOUS CONSTANT LOAD

a) *Compression and elongation apparatus*

An apparatus was made for the short duration test. This was composed of two parts, one of which has two circular metal plates (28.3 cm^2 in surface area) attached to

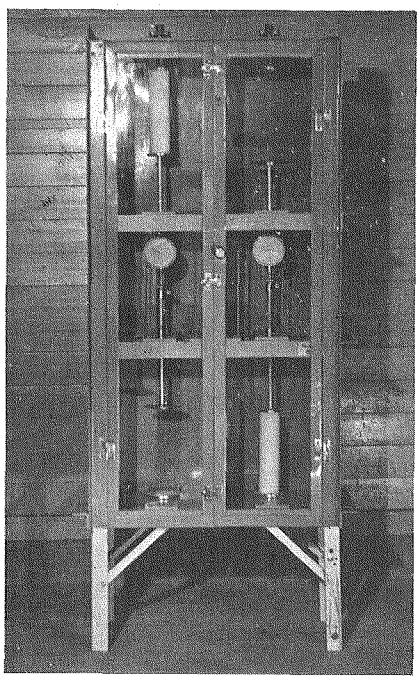

Fig. 1. Compression and elongation apparatus for the tests of minute deformation

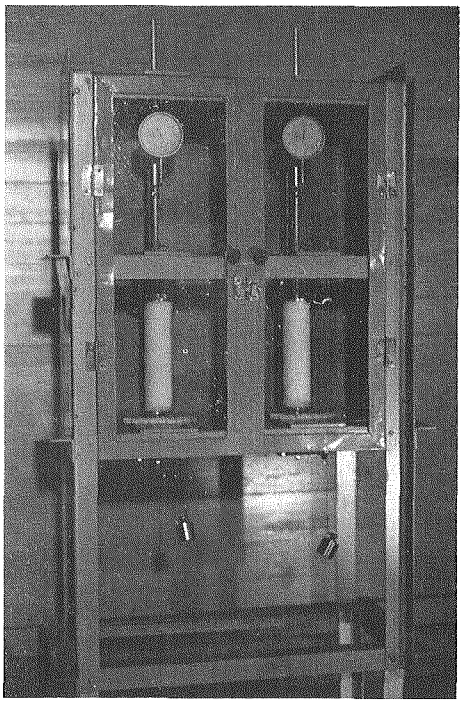

Fig. 2. Torsion test for the test of minute deformation

the upper part to give elongation to the snow sample, while the other also has two plates (20 cm^2) at the lower part, which delivers the compression. Two samples were placed simultaneously on this apparatus in order to measure the compressibility and the extensibility by means of a dial indicator (10^{-2} mm in accuracy) which facilitates the vertical movement and positioning of the plate with the aid of a screw stopper. In the case of compression or elongation for the short duration, a snow sample was placed on the two circular plates at the lower and upper parts; for elongation the sample was frozen to the plates. Then, after weights were mounted on the upper or lower plate connected with a movable shaft, the screw stopper loosened with care.

The apparatus used for the long duration test was equipped with four components, otherwise there was no structural difference between the apparatus for long duration and that for short duration except in the recording devices which has a drum. The deformation of snow sample was recorded on the drum with a pen fixed to the movable shaft. Both apparatuses are shown in Figs. 1 and 2, respectively.

b) *Torsion apparatus*

The torsion apparatus has two components equipped with a circular plate fixed to a movable shaft at the upper end and a rotary circular plate (28.3 cm^2 in sectional area) at the lower end. A string wound around a pulley (6 cm in diameter) fixed parallel with the rotary circular plate on a same axis which was supported by two ball-bearings to make the rotation as smooth as possible, was tied to weights through another small pulley fixed normally at the same level. Torsional deformation was observed by the

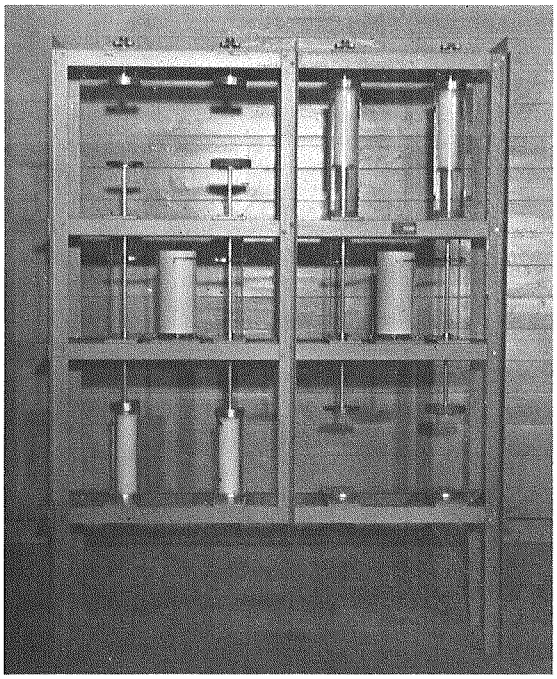

Fig. 3. Compression and elongation apparatus for the long duration test

angle indication of the pointer, fixed to the lower side of the rotary plate. This apparatus is shown in Fig. 3.

Both types of apparatuses were covered with a sheet-iron casing in order to eliminate the effects of temperature fluctuation in the cold room and the formation of frost in the moving parts and the dial indicator. Each sample was protected against evaporation by acrylite cylinder coverings.

2) THE DEVICE FOR THE DEFORMATION TEST UNDER VARIOUS CONSTANT SPEEDS

The device consists of the following parts. Namely three types of deformation apparatus (compression, tension and torsion) of constant speed, a protection housing with three compartments to maintain a controlled temperature of the snow sample and an internally involved simple electric circuit together with an auto-switching box for alternating the order of lead wires which enables switching to the three types of deformation, and a recorder.

Each deformation device has two circular metal plates (28.3 cm^2 in surface area) for setting up the snow sample. Though the upper plate is combined with a shaft chopped up fine ruck in order to transmit the rotary force of the motor, it is movable as a whole smoothly in vertical direction by disconnecting a catch, in order to facilitate the installation of the snow sample. A required constant speed of deformation is selected from 11 kinds in compression or tension, or from 8 kinds in torsion by exchanging a few gears.

On the other hand, each lower plate is fixed to small cases involving load cells (the range of measurement: 20 kg-wt in compression and tension, 2 kg-wt·cm in torsion).

Three time-switches for each test are installed at the lower part of the protection housing and the required deformation period is set. Small front doors in the three

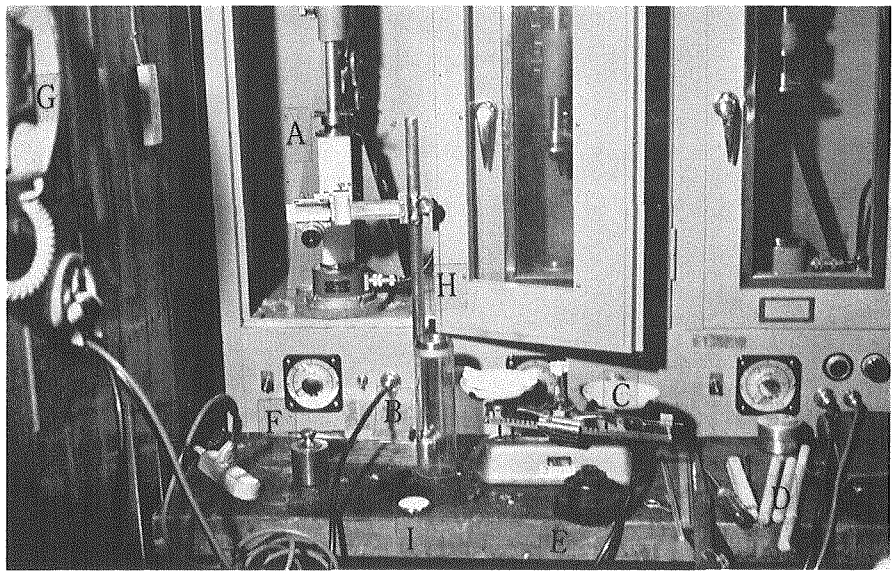

Fig. 4. Apparatus for the compressive, tensile and torsional deformations of each constant speed (assembly view)

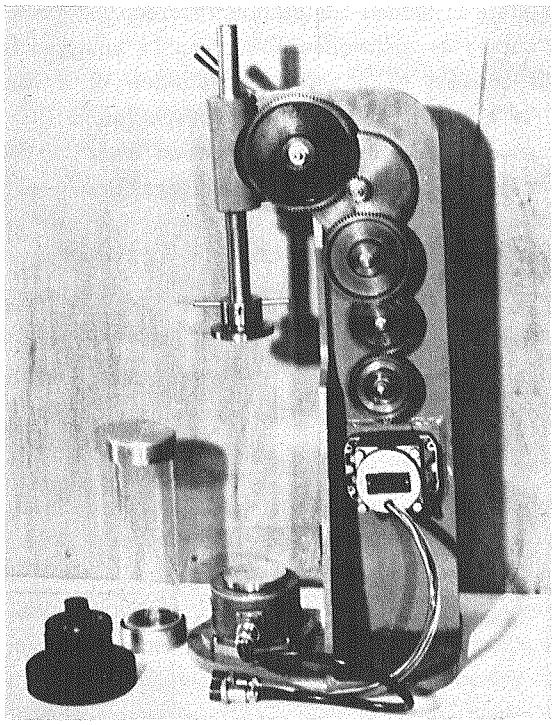

Fig. 5. Apparatus for the compressive deformation of constant speed (sectional view)

boxes in the housing can be removed upwards for placing the snow sample. An assemply view of the experiment in the cold room is shown in Fig. 4 and a sectional view of the apparatus for compressive or tensile deformation is shown in Fig. 5, respectively. The devices in Fig. 4 are as follows.

Three deformation devices of constant speed; several thermometers; a balance for measuring the weight of snow samples; a microscope for measuring the width of snow sample under deformation; a small saw for removing a snow sample from the circular metal plates in tension or torsion at the end of test; some spare gears and pinions for exchange; several weights to check the sensitivities of each load cells; a simple telephone; an acrylite snow sampler and etc.

IV. Measurements and Considerations

1) DEFORMATION TESTS OF CONSTANT LOAD

a) *Results of the short duration tests*

The cross-sectional area of the snow sample remained apparently unchanged with such small axial deformations, so that the stresses were calculated with consideration to this fact. As for the compression of the snow, it has been found already by some research workers (Yosida, 1965; Kojima, 1954, 1955, 1956, 1957, 1958 etc.) that an instantaneous strain was first seen followed by a kind of viscous strain. The strain rate of the latter decreased with lapse of measuring time and approached approximately to a certain

constant value. This state is named the stationary creep.

Such strain-time curves as mentioned above can be analyzed formally by the four-element model which consists of a serial combination of a Maxwell's element and a Voigt's element. As a result of these tests, it was found that the same treatment could be permitted also on the elongation and torsion tests.

The creep motion is expressed by the following relation,

$$e=\frac{P}{\gamma}+\frac{P}{\gamma'}(1-e^{-t/\tau})+\frac{P}{\eta}t\,;\quad \tau=\frac{\eta'}{\gamma'}\,, \tag{1}$$

where e is the strain of the vertical axis or strain of the shear, P is compressive, tensile or shearing stress, η' and γ' are coefficients of viscosity and elasticity related to retardation, γ is the coefficient of elasticity of the strain caused instantaneously, η is the coefficient of viscosity to be obtained from the stationary creep, τ is the retardation time

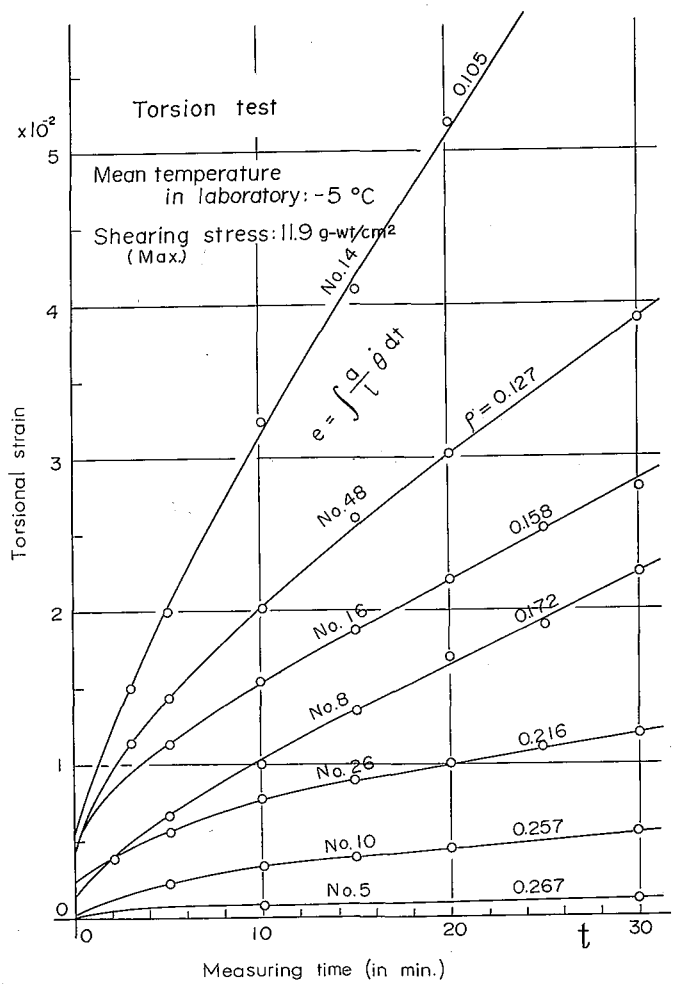

Fig. 6. Strain-time relations in various snow densities under constant torsional load. l, length of sample (cm); a, radius of sample (cm); e, torsional strain; $\dot{\theta}$, angular velocity (rad/min); ρ, snow density (g/cm³)

and t is the measuring time, respectively.

These physical values in each test were measured with many snow samples of different densities. The snow temperature was varied in a range of 0 and -40°C in order to obtain a more precise investigation of the effect of temperature on the coefficient of viscosity for the stationary creep stage.

(i) Creep curves

The changes of strain in time due to the compression, elongation and the torsion were analyzed in comparison with the creep curve of the four-element model. The gradient of each creep curve increases with the stress and the temperature of the snow, and decreases with the density of the snow sample.

Figure 6 shows an example of strain-time relations in the torsion test at -5°C mean test temperature, 11.9 g-wt/cm^2 shearing stress. The strain rates in the stationary creep observed in each test were proportional to the stress and their order of magnitude ranged from 10^{-5} to $10^{-3}\,\mathrm{min}^{-1}$ within the limits of the test conditions.

(ii) The coefficients of elasticity calculated in terms of strain caused instantaneously: γ

Some deformations were observed at the moment when the sample was subjected to vertical or torsional load. The deformation depends not only upon the microscopic texture of the snow sample which is influenced by past history under certain conditions, but also upon the contact area between the circular metal plate and the roughened end of the snow sample, the experimental methods, etc. Thus the determination of γ is most difficult with these instruments. The value of γ increases with the density and decreases with the temperature of the snow sample, but the effect of stress on the value of γ is not apparent here.

(iii) The coefficients of viscosity and elasticity obtained with respect to the retardation elements: η', γ'

In this case the effects of stress are also not so clear, but the values of η', γ' have a tendency to increase as the temperature of the snow sample decreases.

(iv) Retardation time: τ

The ratio of η'/γ', which is called retardation time, was considered to be approximately constant under various test conditions.

(v) The coefficient of viscosity related to the stationary creep: η

The characteristics of the greater part of sample deformation observed during the test period depends upon the coefficient of viscosity. Consequently, the values of η which is important in the investigation of the physical properties of snow, were measured with particular care in a range of 0 and -40°C as aforementioned.

The values η obtained from each test are expressed in terms of exponential functions of the density ρ and the temperature T. The coefficient of viscosity η was found to be the smallest in shearing, medium in compression and the largest in elongation. Table 1 shows the formulae computed by the aid of the figures corresponding to the three types of test.

Figure 7 expresses the relation between the density of the snow sample and the coefficient of viscosity η_c resulting from the stationary creep in the compression test of short duration.

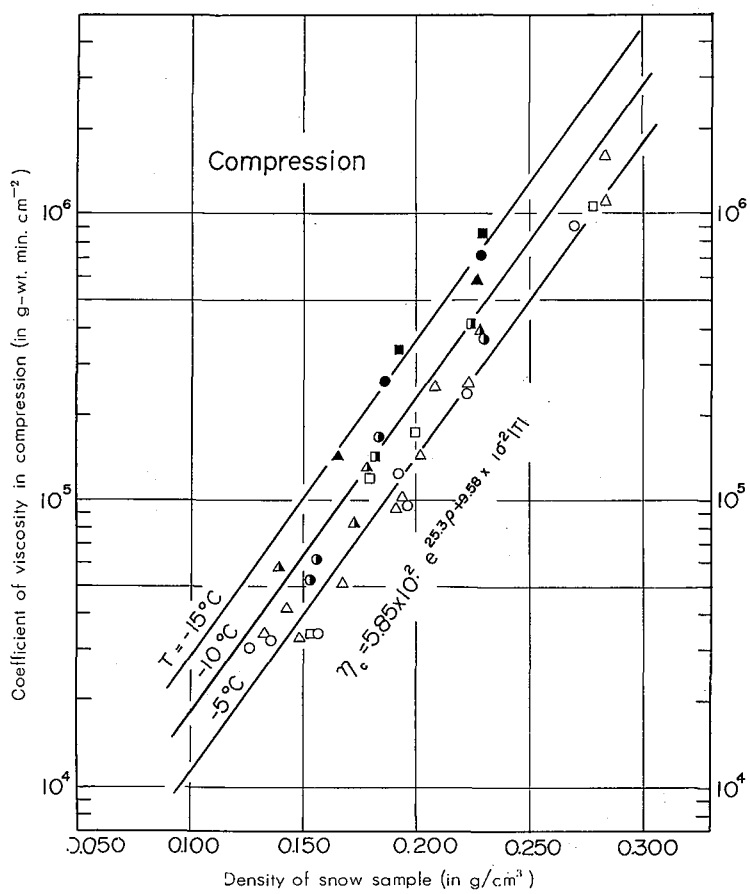

Fig. 7. Relations between the coefficient of viscosity and the density of snow sample in compression of short duration, under constant and uniaxial load

Table 1. The coefficients of elasticity and viscosity computed approximately from the process of each deformation at −5°C except for the value of η

Deformation	γ (g-wt/cm^2)	γ' (g-wt/cm^2)	η' (g-wt·min/cm^2)	η (g-wt·min/cm^2)	τ (min)
Torsion	$0.52\times10^2\,e^{25.3\rho}$	$0.64\times10^2\,e^{25.3\rho}$	$0.35\times10^3\,e^{25.3\rho}$	$2.88\times10^2\,e^{25.3\rho+9.58\times10^{-2}\lvert T\rvert}$	5.04
Compression	$1.24\times10^2\,e^{25.3\rho}$	$2.10\times10^2\,e^{25.3\rho}$	$1.07\times10^3\,e^{25.3\rho}$	$5.85\times10^2\,e^{25.3\rho+9.58\times10^{-2}\lvert T\rvert}$	4.92
Elongation	$1.84\times10^2\,e^{25.3\rho}$	$1.91\times10^2\,e^{25.3\rho}$	$0.95\times10^3\,e^{25.3\rho}$	$9.39\times10^2\,e^{25.3\rho+9.58\times10^{-2}\lvert T\rvert}$	5.30

ρ: Density of snow sample (in g/cm^3), T: Temperature of snow sample (in °C).

Figure 8 expresses the relation between the temperature of snow sample and η_c.

b) *Results of the long duration tests*

A lateral deformation of the snow sample was observed in the long duration test. It shows that the internal stresses produced by the weight of the sample itself and the constant uniaxial load, changed as the deformation progressed.

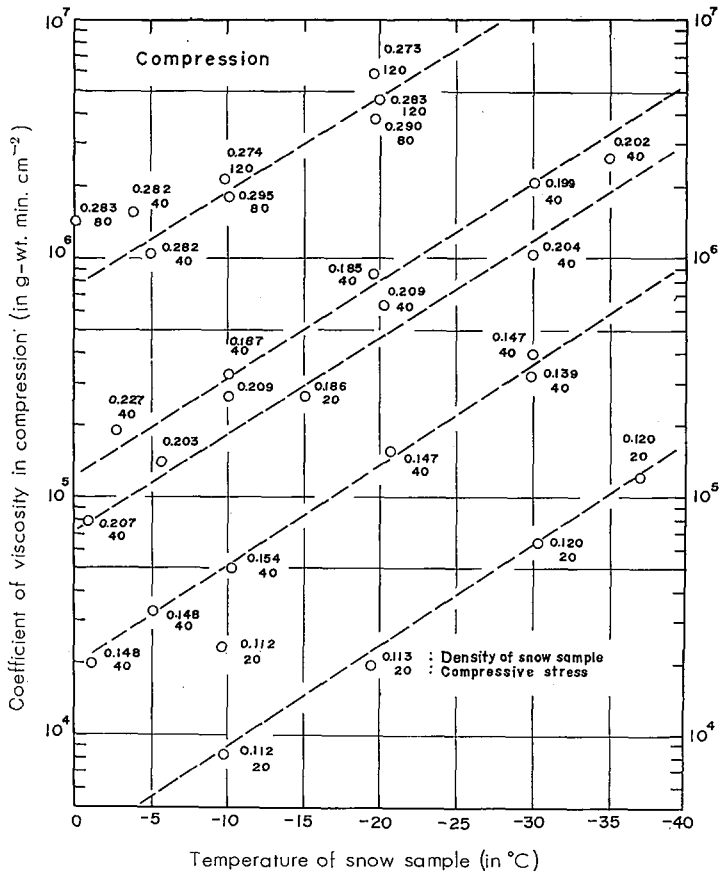

Fig. 8. Relations between the coefficient of viscosity resulting from the stationary creep and the temperature of snow sample in compression

(i) Strain-time curves

From the long duration tests, the data for compression and elongation were collected. The strain resulting from each test increases smoothly with the measuring time and it was shown that the larger the density, the smaller the strain under the same initial stress. However, the strain rate decreases gradually and a uniform creep does not occur. Since the strain in compression is larger than in elongation, it seems that the snow behaves with more resistance to the latter test than to the former.

(ii) Poisson's ratio: σ

The lateral expansion and contraction of the snow sample are proportional to the compressive and tensile strains. The relation between the sample diameter and the axial compressive or tensile strain is expressed by the following equations.

$$\int_{d_i}^{d_t} \frac{dD}{D} = -\sigma \int_{l_i}^{l_t} \frac{dL}{L},$$

$$d_t = d_i (l_i/l_t)^{\sigma}$$

$$= d_i e^{-\sigma e_v} \fallingdotseq d_i (1-\sigma e_v), \qquad (2)$$

where d_i and d_t are sample diameters measured at the initial time and time t, l_i and l_t are sample lengths at the time of measuring the diameter, σ is Poisson's ratio, e_v is the vertical strain.

The over all mean values of σ computed are given as follows,

$$\bar{\sigma}_c = 0.03 \quad \text{in compression,}$$
$$\bar{\sigma}_e = 0.49 \quad \text{in elongation.}$$

Since the lateral contraction was remarkable in elongation, no volume change practically took place there and consequently the sample density can be regarded as constant during the test, disregarding the weight reduction or expansion on the diameter of each snow

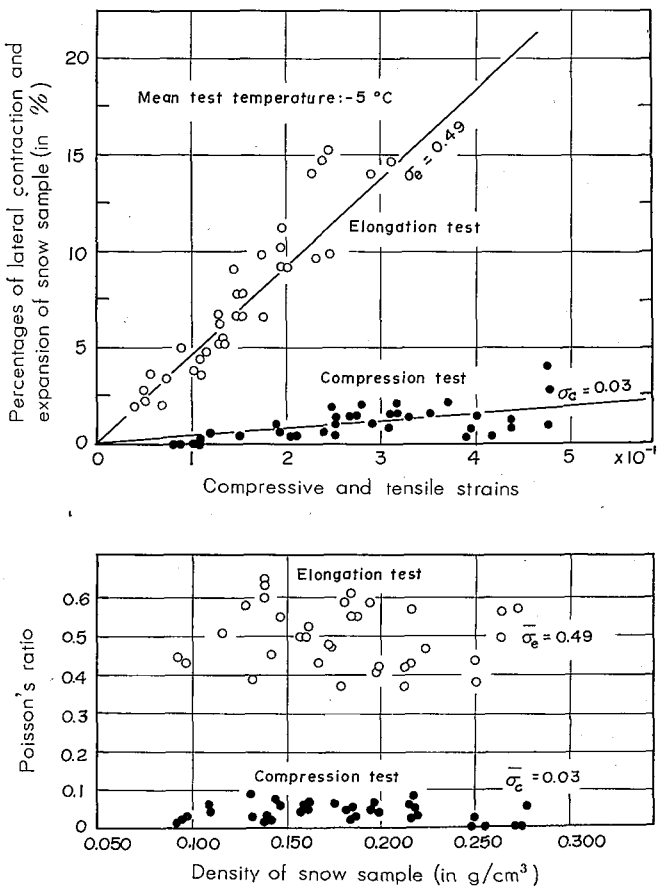

Fig. 9. Changes of the diameter of sample according to the vertical strain and the distribution of Poisson's ratio in relation to the density of snow sample

sample resulting from verticel strains and the distribution of Poisson's ratio in relation to the density of snow sample are illustrated in Fig. 9, respectively.

(iii) Hardening of the snow sample

Figure 10 represents the coefficient of viscosity changing with the test time during the long tensile process and Fig. 6 expresses the relation between the coefficient of

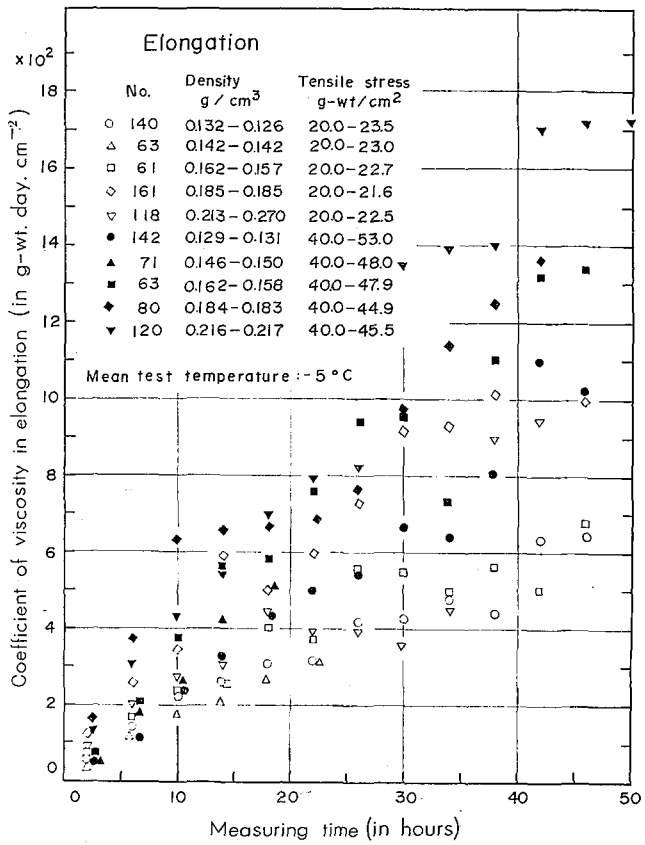

Fig. 10. Changes of the coefficient of viscosity during tensile process

viscosity in elongation and the density of snow sample, respectively. As shown in Fig. 11, it was found that the snow of the same density can take various coefficients. This value is called the apparent coefficient of viscosity η_a, because this gives the ratio of internal stress to the corresponding strain rate with the test time, in long duration and it remarkably exceeds the values gained by small deformation at the same density of the snow sample. This phenomenon is designated here as hardening and is generally more remarkable in elongation than in compression. The larger the initial density of the sample and the load applied, the more the rate of hardening phenomenon increases. Particularly, the extensibility of the snow sample in the elongation test becomes gradually smaller in spite of the momentarily increased tensile stress, owing to the remarkable lateral contraction of the sample during the test. This result coincides with that reported by Haefeli in 1939 (1954, Translation, Chapter II. Part 1, pp. 57–127). Yosida (1948) reported a simple linear relation between the compressive creep rate and the density of snow on the basis of the results of his experiment on minor compression of cylindrical snow samples under constant loads. Kojima (1954), on the densification-process of snow deposited horizontally and Shinojima (1962), on the three types of small deformations (compression, elongation and torsion) with cylindrical snow samples,

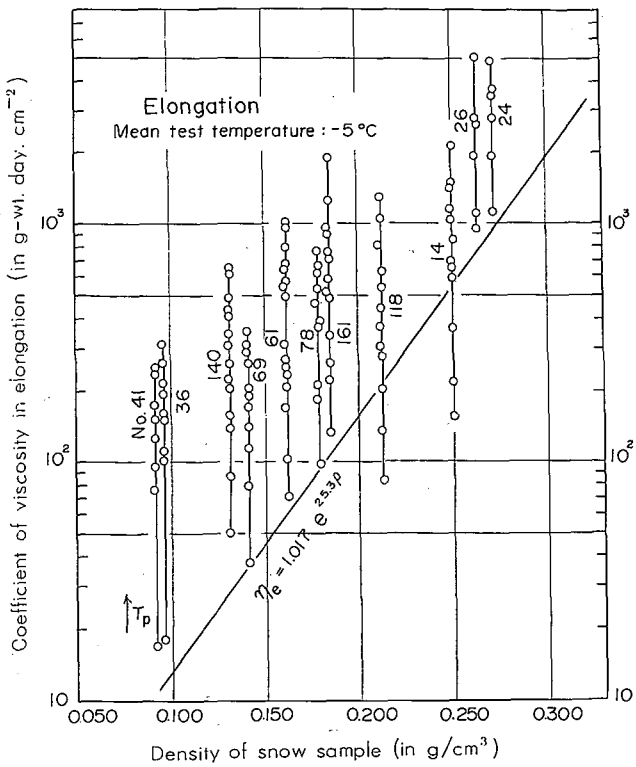

Fig. 11. Relations between the coefficient of viscosity and the density of snow sample in the elongation test of long duration

respectively found that the relation between the density of snow and the coefficient of viscosity in stationary state was determined uniquely by means of an exponential function.

However, the mechanical state of a snow cover can be created generally under various combinations of two phenomena. The first is the softening phenomenon such as the recrystalization according to a particular temperature gradient in a snow cover, the vaporization of ice-particles and ice-bonds, the destruction of snow structure by internal stresses, the erosion of snow surface and the steady deposition under certain conditions of wind and the transition to coarse grain by thawed water. The second is the transition to coarse grain by sintering and freezing of thawed water, the volume decrease by own weight, the compacting of the snow surface by such external forces as wind, etc. and the strengthening of ice-bonds by condensation of water vapor etc. Therefore, it is considered that the abnormal hardening or softening of snow may develope when natural conditions of physical factors are disturbed by topographical and meteorological factors or constructions on the ground etc.

c) *Correlations among the values obtained separately from the tests of short and long durations*

(i) η_s computed from the theoretical relations among the coefficients of visco-elasticity.

The three types of coefficients of viscosity η_c, η_e and η_s which were obtained

separately in the short duration test and the average values of Poisson's ratio σ_c and σ_e which were actually measured in the corresponding long duration test can be related with each other by analyzing the small deformation in torsion. When the snow sample is twisted under a certain constant load, the deformations of any small parts in a snow sample fixed in a vertical direction can be considered as pure shear. As shown in Fig. 12, small rectangular parallelpiped inside the snow sample may be subjected to a shearing deformation by shearing stress P_s. This strain of shear e_s can be divided respectively into compressive strain e_c and tensile strain e_e on the directions of two diagonal lines in this small prism.

Thus, three strains and strain rates are related as following in the small shearing

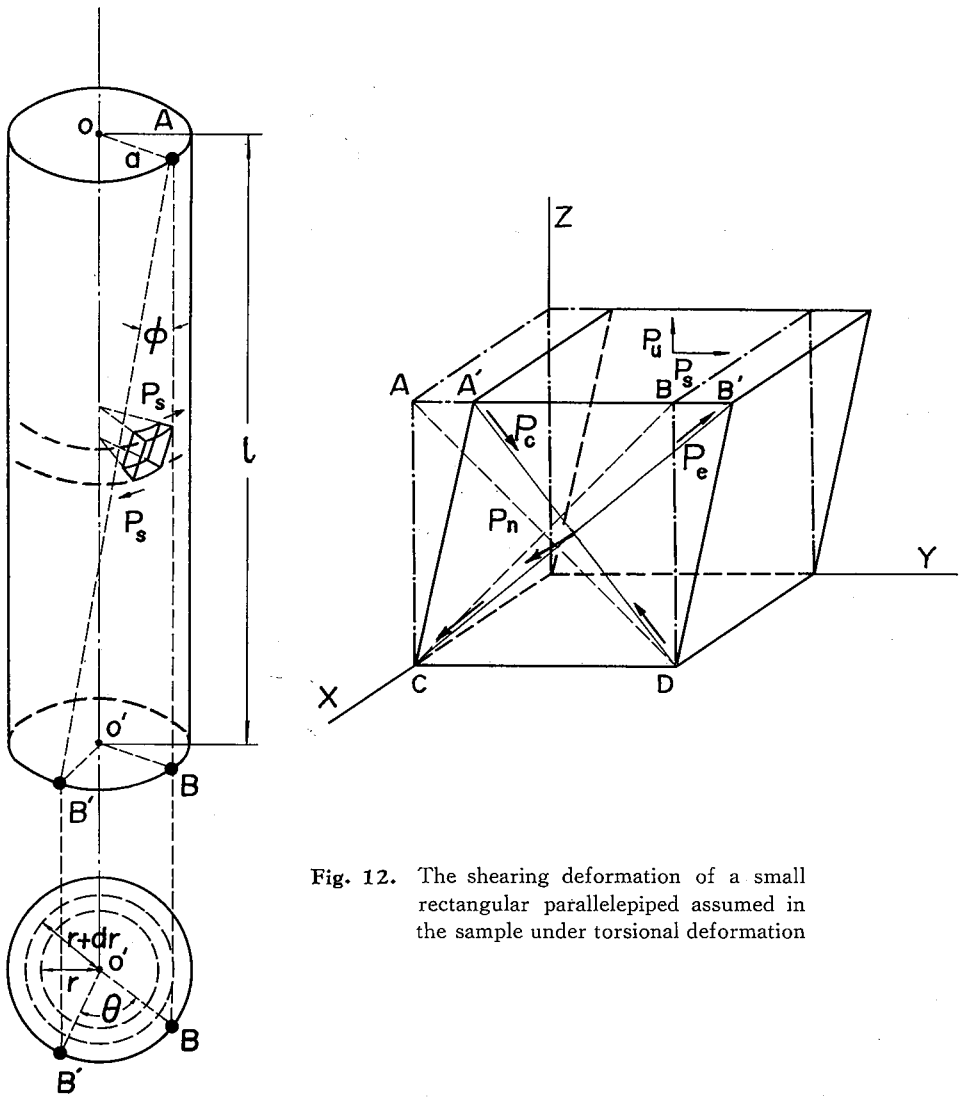

Fig. 12. The shearing deformation of a small rectangular parallelepiped assumed in the sample under torsional deformation

deformation,

$$-e_c = e_e = \frac{e_s}{2}, \qquad -\dot{e}_c = \dot{e}_e = \frac{\dot{e}_s}{2}. \tag{3}$$

Since the snow sample is fixed in a vertical direction during the test, it was considered that tensile stress P_u must be created in the z-direction in Fig. 12, because if P_u is assumed to be absent, the absolute value of P_c and P_e may be equal to each other and the above equation can not hold as far as η_c is not η_e. Therefore, the relations of the stresses corresponding to each strain, P_c, P_e and P_s are obtained as following,

$$\begin{aligned} P_s &= \frac{P_e - P_c}{2}, & & P_c = P_u - P_s, \\ & & \text{or} & \\ P_u &= \frac{P_c + P_e}{2}, & & P_e = P_s + P_u. \end{aligned} \tag{4}$$

On the other hand, the strain rate in shear can be expressed by the definition as follows.

$$\dot{e}_s = \frac{P_s}{\eta_s}. \tag{5}$$

Generally, the relation between the strain and the stress for a complete elastic body is shown by the following equation.

$$e_{rs} = \frac{1+\sigma}{\gamma} P_{rs} - \frac{\sigma}{\gamma} \delta_{rs} P_{\alpha\alpha}; \ r, s : 1, 2, 3, \tag{6}$$

where, e_{rs} and P_{rs} are the strain and stress components, respectively, and $P_{\alpha\alpha}$ is equal to $P_{11}+P_{22}+P_{33}$. It was assumed that the above equation may also hold for the deformation of visco-elastic material.

In the case of torsional deformation likewise lateral deformation of the snow sample during test may be observed as same as in the cases of compression and elongation, and the existence of the stress P_n and the strain rate $\dot{e}_n$ in a lateral direction of the snow sample n and furthermore, the coefficient of viscosity and Poisson's ratio corresponding to that direction are expressed here as η_n and σ_n.

On the three principal directions of stresses, each strain rate and stress are expressed from eq. (5) as follows.

$$\begin{aligned} \dot{e}_c &= \frac{P_c}{\eta_c} - \sigma_e \frac{P_e}{\eta_e} - \sigma_n \frac{P_n}{\eta_n}, \\ \dot{e}_e &= \frac{P_e}{\eta_e} - \sigma_c \frac{P_c}{\eta_c} - \sigma_n \frac{P_n}{\eta_n}, \\ \dot{e}_n &= \frac{P_n}{\eta_n} - \sigma_c \frac{P_c}{\eta_c} - \sigma_e \frac{P_e}{\eta_e}. \end{aligned} \tag{7}$$

1. In the case of the lateral stress $P_n = 0$.

Each stress acting on a small prism is computed from eqs. (3), (4), (5) and (7) as,

$$\begin{aligned} P_c &= \frac{1-\sigma_e}{2(1-\sigma_c\sigma_e)} \frac{\eta_c}{\eta_s} P_s, \\ P_e &= \frac{1-\sigma_c}{2(1-\sigma_c\sigma_e)} \frac{\eta_e}{\eta_s} P_s, \end{aligned} \tag{8}$$

$$P_u = \frac{(1-\sigma_c)\eta_e-(1-\sigma_e)\eta_c}{(1-\sigma_c)\eta_e+(1-\sigma_e)\eta_c} P_s ,$$

$$P_s = \frac{(1-\sigma_e)\eta_c-(1-\sigma_c)\eta_e}{4(1-\sigma_c\sigma_e)} P_s .$$

From the eqs. (5) and (8), the relation of η_c, η_e and η_s are also shown as follows,

$$\eta_s = \frac{(1-\sigma_e)\eta_c+(1-\sigma_c)\eta_e}{4(1-\sigma_c\sigma_e)} . \tag{9}$$

On the other hand, the strain rate of lateral direction $\dot{e}_n$ is written by calculating the above equation.

$$\dot{e}_n = -\frac{\sigma_e-\sigma_c}{2(1-\sigma_c\sigma_e)} \frac{P_s}{\eta_s} . \tag{10}$$

Taking the ratio of P_c and P_e,

$$\left|\frac{P_e}{P_c}\right| = \frac{\eta_e/(1-\sigma_e)}{\eta_c/(1-\sigma_c)} . \tag{11}$$

2. In the case of strain rate in lateral direction $\dot{e}_n=0$.

By calculating each stress in the same manner as above,

$$\begin{aligned}
P_c &= \frac{\sigma_e(1+2\sigma_n)-1}{2\{1-\sigma_n(\sigma_c+\sigma_e)-\sigma_c\sigma_e(1+2\sigma_n)\}} \frac{\eta_c}{\eta_s} P_s ,\\
P_e &= \frac{1-\sigma_c(1+2\sigma_n)}{2\{1-\sigma_n(\sigma_c+\sigma_e)-\sigma_c\sigma_e(1+2\sigma_n)\}} \frac{\eta_e}{\eta_s} P_s ,\\
P_n &= \frac{\sigma_e-\sigma_c}{2\{1-\sigma_n(\sigma_c+\sigma_e)-\sigma_c\sigma_e(1+2\sigma_n)\}} \frac{\eta_n}{\eta_s} P_s ,\\
P_s &= \frac{\eta_c\{1-\sigma_e(1+2\sigma_n)\}+\eta_e\{1-\sigma_c(1+2\sigma_n)\}}{4\{1-\sigma_n(\sigma_c+\sigma_e)-\sigma_c\sigma_e(1+2\sigma_n)\}} \dot{e}_s .
\end{aligned} \tag{12}$$

The relations of η_c, η_e and η_s from the eqs. (5) and (12) are expressed as,

$$\eta_s = \frac{\eta_c\{1-\sigma_e(1+2\sigma_n)\}+\eta_e\{1-\sigma_c(1+2\sigma_n)\}}{4\{1-\sigma_n(\sigma_c+\sigma_e)-\sigma_c\sigma_e(1+2\sigma_n)\}} , \tag{13}$$

and then taking the ratio of P_c and P_e as the same as before, the following relation is obtained,

$$\left|\frac{P_e}{P_c}\right| = \frac{\eta_e/\sigma_e(1+2\sigma_n)-1}{\eta_c/\sigma_c(1+2\sigma_n)-1} , \tag{14}$$

where, the values of σ_n, η_n and $\dot{e}_n$ are Poisson's ratio, the coefficient of viscosity and strain rate respectively obtained from the positive or negative value of P_n.

When $P_n>0$ (tensile stress): $\sigma_n=\sigma_e$, $\eta_n=\eta_e$, $\dot{e}_n<0$.

When $P_n<0$ (compressive stress): $\sigma_n=\sigma_c$, $\eta_n=\eta_c$, $\dot{e}_n>0$.

In the eqs. (9) and (13), putting $\eta_c=\eta_e=\eta$ and $\sigma_c=\sigma_e=\sigma_n=\sigma$, the general relation of viscosity between shear and elongation deformation can be obtained as,

$$\eta_s = \frac{\eta}{2(1+\sigma)} . \tag{15}$$

3. Numerical calculation

Assumption 1: The lateral stress $P_n=0$.

Each stress in shearing deformation is obtained from eq. (8) by substituting the values of the corresponding stress, coefficient of viscosity and Poisson's ratio.

$$P_c = -0.522\ P_s < 0\,,$$
$$P_e = 1.60\ P_s > 0\,,$$
$$P_u = 0.508\ P_s > 0\,.$$

It is found that P_u is a positive value and therefore the tensile stress, and the relation of the three stresses in eq. (4) is held with good approximation.

The ratio of P_c and P_e is as follows from eq. (11),

$$\left|\frac{P_e}{P_c}\right| = 3.07\,.$$

Namely, the tensile stress is about three times that of the compressive stress under assumption without lateral stress. The strain rate $\dot{e}_n$ is computed by eq. (10) as,

$$\dot{e}_n = -0.234\,\frac{P_s}{\eta_s} < 0\,.$$

This value is negative and therefore, it is the strain rate according to compression. Consequently, the snow sample in torsion must be contracted lateraly, when the lateral stress P_n does not act on it. The coefficient of viscosity η_s is computed by means of eq. (9). Namely,

$$\eta_s = 3.60\times 10^2 \varepsilon^{25.3\rho + 9.58\times 10^{-2}|T_1|}\,,$$

and by substituting η_s measured actually into this eq. (9), Poisson's ratio in compression is obtained as,

$$\sigma_c = 0.052\,.$$

This value coincides approximately with the average value $\bar{\sigma}_c$ resulting from the long duration test.

Assumption 2: Strain rate of lateral direction $\dot{e}_n = 0$.

According to the result of $\dot{e}_n$ derived from assumption 1, P_n must be taken as the positive value and therefore, the values of η_n and σ_n will become η_e and σ_e respectively.

Each stress is as follows in the results of computation.

$$P_c = -0.026\ P_s < 0\,,$$
$$P_e = 2.15\ P_s > 0\,,$$
$$P_n = 1.06\ P_s > 0\,.$$

The ratio of P_c and P_e is

$$\left|\frac{P_e}{P_c}\right| = 83.5\,,$$

and when the lateral tensile stress is assumed to be acting on the same sample the contribution of shearing stress P_s will be limited only to the inducement of tensile stress.

The coefficient of viscosity η_s can be obtained by calculating eq. (13).

$$\eta_s = 3.14\times 10^2 \varepsilon^{25.3\rho + 9.58\times 10^{-2}|T_1|}\,.$$

Thus, η_s should be obtained theoretically as the value between the two computed results from eqs. (9) and (13). However, the value of η_s observed practically is a little smaller

than both computed values; *i.e.*, 2.88×10^{2} which is the value of η_s shown in Table 1 corresponding to $\rho=0$.

(ii) Poisson's ratio computed from the theoretical relations among the coefficients of visco-elasticity.

The coefficients of visco-elasticity in the four-element model expressed by creep eq. (1) can be obtained separately from each test, the ratio between the values of which can be expressed approximately as follows for the sake of simple consideration hereafter.

		Shear		Compression		Elongation
Maxwell's element	τ	1	:	2	:	3
	η	1	:	2	:	3
Voigt's element	τ'	1	:	3	:	3
	η'	1	:	3	:	3

Thus, creep eq. (1) can be rewritten in the following equations according to the approximate values from the above table.

$$e_e = aP_e\varepsilon^{\alpha\rho}\left\{1+b(1-\varepsilon^{-t/\tau})+ct\right\},$$

$$e_c = 2aP_c\varepsilon^{\alpha\rho}\left\{1+\frac{3}{2}b(1-\varepsilon^{-t/\tau})+ct\right\},$$

$$e_s = 3aP_s\varepsilon^{\alpha\rho}\left\{1+b(1-\varepsilon^{-t/\tau})+ct\right\}.$$

where, suffix e, c or s means the type of deformation, ρ is the snow density, the values of a, b, c, α, τ are constants determined by each test and their average values are obtained as $a=1.72\times10^{-2}$ cm^2/g-wt, $b=8.88\times10^{-1}$, $c=1.26\times10^{-1}$ min^{-1}, $\alpha=-2.53\times10^{-1}$ cm^3/g and $\tau=5.18$ min, respectively.

1. On mechanical constants related to Voigt's element.

As known from the above table, there are the following relations on the coefficients of visco-elasticity in Voigt's element, $\tau'_c=\tau'_e$ and $\eta'_c=\eta'_e$. Namely, in consideration to the small deformation of deposited snow, both contributions of compression and elongation to the mechanical constants related to Voigt's element are identical with each other and therefore, it may be estimated that only the coefficients of visco-elasticity related to Maxwell's element are different in the two types of deformation.

The mechanical constants related to Voigt's element can be written as follows, by using the general relation (15) among the coefficients of visco-elasticity of shear and elongation.

$$\tau'_s = \frac{\tau'_c}{2(1+\sigma'_c)} = \frac{\tau_e}{2(1+\sigma'_e)},$$
$$\eta'_s = \frac{\eta'_c}{2(1+\sigma'_c)} = \frac{\eta'_e}{2(1+\sigma'_e)}. \qquad (16)$$

If the values of σ'_c and σ'_e are here taken as 0.5 respectively, the relations of each coefficient in the above two equations coincide with the results in the above approximate table and can be rewritten in the following simple forms.

$$\tau_{s'} = \frac{\tau'_c}{3} = \frac{\tau'_e}{3}, \quad \eta'_s = \frac{\eta'_c}{3} = \frac{\eta'_e}{3}.$$

Consequently, some part of the snow structure related to the retardation phenomenon acts as the same in both deformations of compression and elongation and furthermore as if like being $\sigma'_c=\sigma'_e=0.5$ for Poisson's ratio of that part.

2. On mechanical constants related to Maxwell's element.

By using here again the general relation (15), each coefficient of visco-elasticity related to Maxwell's element can be shown formally as follows.

$$\gamma_s=\frac{\gamma_c}{2(1+\sigma_c)}=\frac{\gamma_e}{2(1+\sigma_e)},$$
$$\eta_s=\frac{\eta_c}{2(1+\sigma_c)}=\frac{\eta_e}{2(1+\sigma_e)}. \tag{17}$$

According to the values in the above ratio-table, Poisson's ratio in relation to Maxwell's element must be taken to be $\sigma_e\fallingdotseq 0.5$ and $\sigma_c\fallingdotseq 0$. Namely,

$$\gamma_s=\frac{\gamma_c}{2}=\frac{\gamma_e}{3},\qquad \eta_s=\frac{\eta_c}{2}=\frac{\eta_e}{3}.$$

These results permit the average values of Poisson's ratio $\bar{\sigma}_e=0.49$ and $\bar{\sigma}_c=0.03$ observed practically and separately in compression and elongation tests of long duration.

However, according to above two discussions, there is no precise interpretation concerning which part in the internal structure of deposited snow, subjected to some deformations, acts as the motion of Maxwell's element or Voigt's element. The mechanical anisotropy of the snow structure which is observed in the difference between the deformation in compression and elongation, is thought to be due to the behavior of snow structure in relation to Maxwell's element.

2) DEFORMATION TESTS OF CONSTANT SPEED

a) *Stress-time relations*

The increasing features of compressive, tensile and shearing stresses which were observed on the snow sample subjected to corresponding deformations of constant speed were very similar to each other. It was found by measurements that the steep and linear stress increase resulting from the elastic deformation was brought about during a short time at the beginning of the deformation and then it was followed by a steady and increasing curve for viscous deformation having the small unevenness of stress resulting probably from small fractures in the internal structure of the snow sample. This increasing rate of stress may depend particularly on the velocity of deformation supplied to the sample.

The general effects of stress increase and relaxation corresponding to each velocity of deformation are shown schematically in Fig. 14. These increasing or decreasing states of stress are explained as follows on the whole. Consequently, it is considered that the changing rate of stress may depend not only on the velocity of deformation, but also on the density and the temperature of the snow sample.

Type A.

Though a sample subjected to a certain extent of deformation speed was destroyed, the stress-curve observed thereafter was that of a serial serration. When the velocity

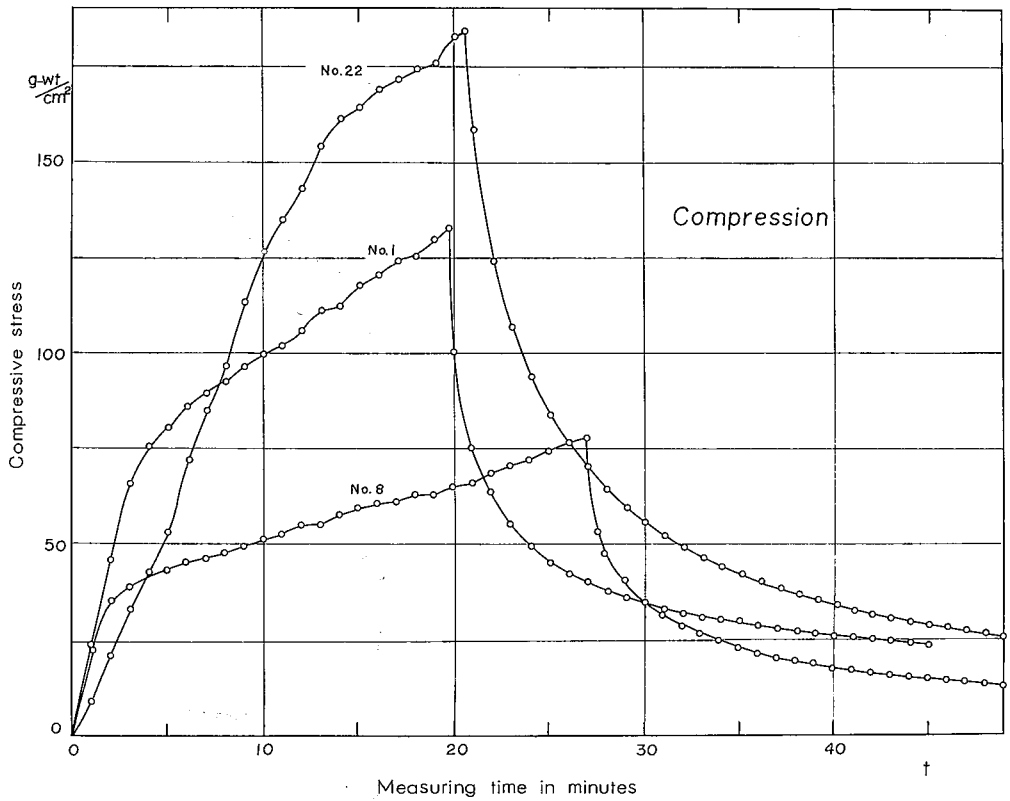

Fig. 13. Examples of the stress-time relation observed from various compressive deformations of constant speed

of deformation is comparatively large, the stress increases rapidly and during viscous deformation, it will be represented as an increasing concave curve having many small jaggednesses. On the contrary, if the velocity of deformation is small, this curve will appear as an increasing convex curve. Whereas the rates of relaxation of the snow samples subjected to deformation due to relatively large speed will be also large, the stress relaxations will be represented as a rapidly and currently decreasing curve in the initial part after the stop of deformation.

Type B.

The stress conditions for a single sample subjected discretely to the same quantity of strain every certain time interval are also shown schematically. In the course of the test, the stored stress at the first deformation was not relaxed completely during the stop period of deformation, and the sample underwent the next deformation and was repeated thereafter. Therefore, each maximal stress obtained at the stop of each discrete deformation becomes gradually large, but the change of sample density resulting from total accumulated deformation at each deformation period was neglected.

Type C.

Under a few suitable combinations between the deformation speed and the deformation period, if the total strains obtained respectively are equal to each other, it will

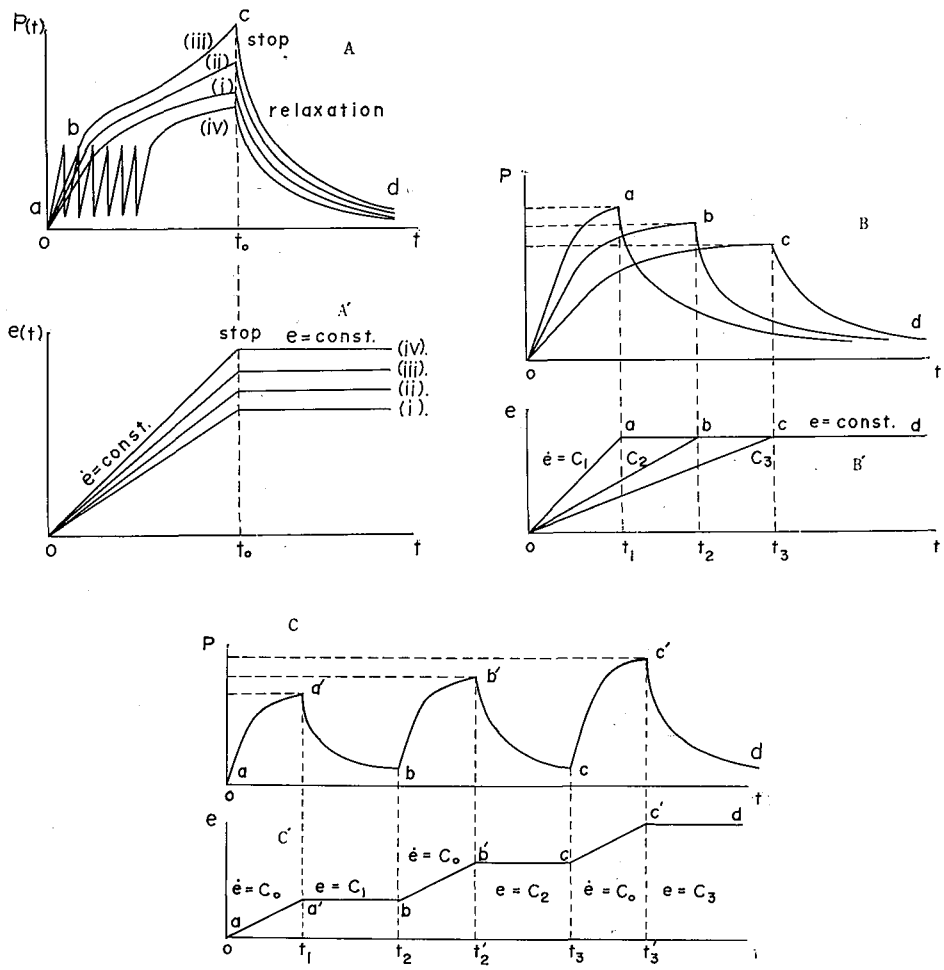

Fig. 14. General behaviors of the stress-time relations corresponding to each deformation of constant speed

be found that the larger the deformation speeds, the larger the stresses corresponding to the strain of the same quantity and the rate of relaxation.

b) *Properties of the coefficient of elasticity*

The coefficient of elasticity computed from tangential lines on each initial part of the stress-time curves which are considered to be due to elastic deformation can be characterized by some experimental factors (strain rate, temperature and density of snow sample, etc.). Figure 15 shows the relation between the coefficient of elasticity and the strain rate. Each point illustrated was decided by its position according to the density and the temperature of the snow sample, respectively, and it was assumed that the relations between the coefficient of elasticity and the strain rate are expressed uniquely by the lines binding only the points with similar values of temperature and density.

Taking the average of the gradients of all linear lines, the relation between both values can be represented as follows.

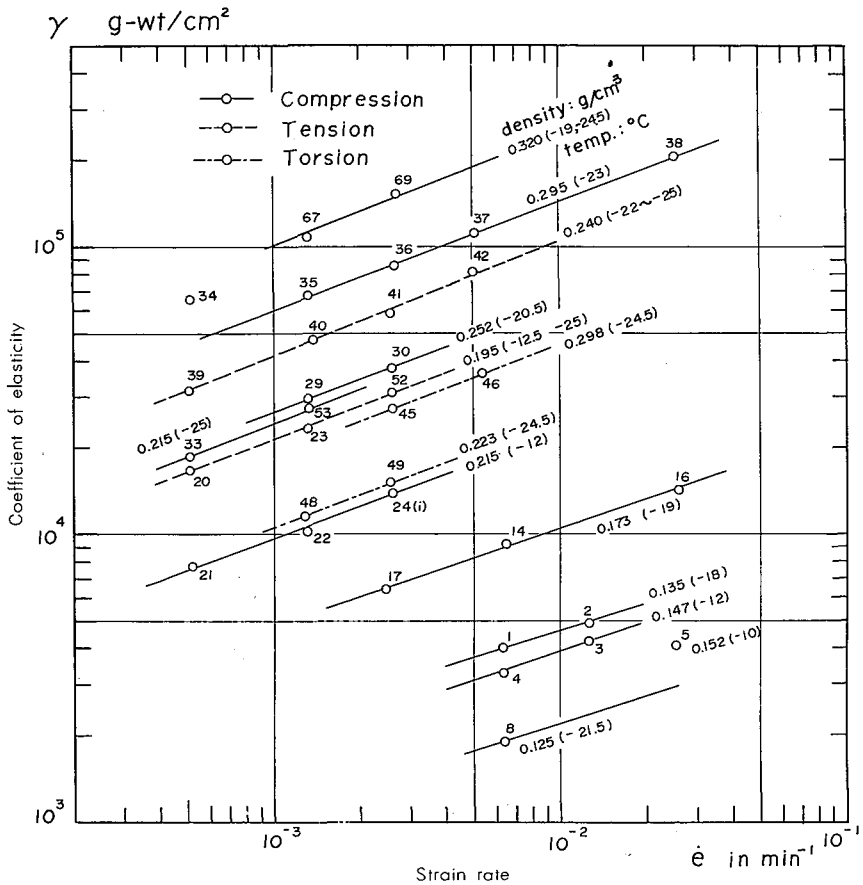

Fig. 15. Dependency of the coefficient of instantaneous elasticity on the strain rate

$$\log \gamma = 0.380 \log \dot{e} + \mathrm{f}(T, \rho)\,, \tag{18}$$

where γ is the coefficient of elasticity, $\dot{e}$ is the strain rate, T and ρ are the temperature and density of the snow sample, respectively.

It is assumed from Fig. 15 that the second term of the right hand side in the above equation, f will be decided by the temperature and the density of the snow sample. Accordingly, the temperature dependency of the values related to the coefficient of elasticity and the strain rate is shown in Fig. 16 by taking the magnitude of $\gamma/\dot{e}^{0.380}$ on ordinate and the absolute values of temperature on abscissa in logarithmic scales, respectively. According to the graph, it may be found by binding the points similar in density between both logarithmic values that there is a linear relation with the same gradient.

It is considered that the differences among each linear relation may depend on the density of the snow sample. Namely, the linear relation is obtained as,

$$\log \gamma/\dot{e}^{0.380} = 0.651 \log T + g(\rho)\,. \tag{19}$$

In order to characterize the second term of the right hand side in the above equation

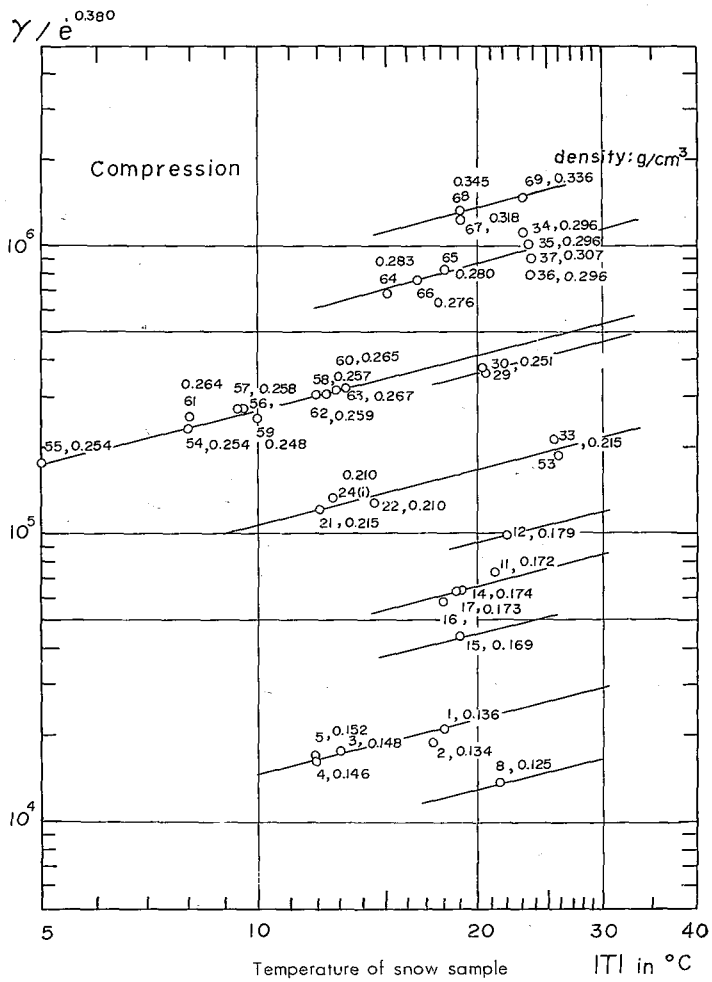

Fig. 16. Relations between the values computed from the coefficient of elasticity and the strain rate, and the temperature of snow sample

g, the values related to γ, $\dot{e}$ and T on ordinate and the density of snow sample on abscissa are shown in logarithmic scale in Fig. 17. According to this figure, there are the differences in three types of deformation (compression, tension and torsion) in the relation among γ, $\dot{e}$, T and ρ.

Their relations are expressed as follows.

$$\gamma_i = A_i \dot{e}^{0.380} |T|^{0.651} \rho^{4.98} = A_i \dot{e}^{\frac{3}{5}} |T|^{\frac{2}{3}} \rho^5 \; ; \quad i = t, \; c \text{ or } s, \tag{20}$$

where suffix t, c or s means the type of deformation, *i.e.*, tension, compression or shear, respectively.

$$A_t = 8.84 \times 10^7, \quad A_c = 5.54 \times 10^7, \quad A_s = 2.82 \times 10^7.$$

Accordingly, the ratios among the three coefficients of elasticity are shown as,

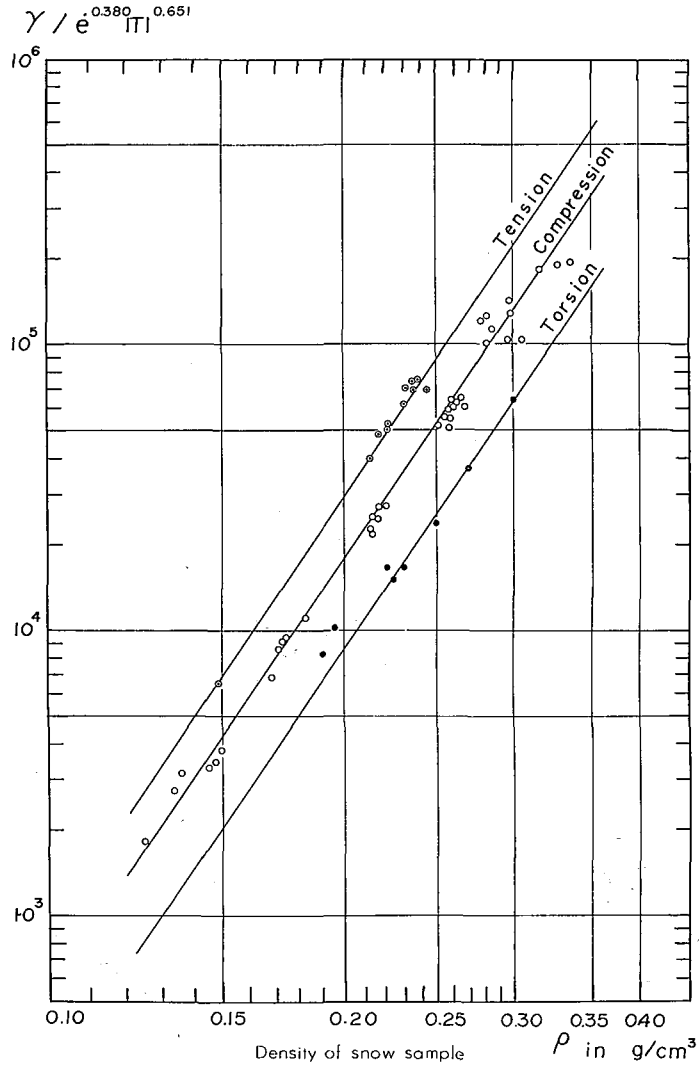

Fig. 17. Relations between the values computed from the coefficient of elasticity, the strain rate and the temperature of snow sample, and the density of snow sample on the three types of deformations

$$\gamma_s : \gamma_c : \gamma_t = 1 : 1.96 : 3.06 .$$

It is considered that these differences may depend on the mechanical unisotropy of snow inasmuch as the cases were investigated in the tests with a static load and therefore Poisson's ratios in the compression and tension may be different.

c) *Approximation of the stress relaxation*

The stress relaxation in all cases after the stop of deformation under constant speed were represented uniformly as a monotonously decreasing curve and therefore, they could be expressed by some exponential equations.

Actually, the relaxation curves gained from the three types of deformation were approximated here by the following equation,

$$P(t)=\left\{P(t_0)-P_0\right\}\varepsilon^{-\beta(t-t_0)^{\alpha}}+P_0\,;\quad t\leq t_0,\ \tau=1/\beta^{1/\alpha}\,, \tag{21}$$

where $P(t)$ and $P(t_0)$ are the compressive, tensile or shearing stress at time t and at the time t_0 of each corresponding deformation, respectively. α and β are numerical values which will be expressed as a function of the experimental factors. τ is the time indicating the extent of relaxation. The above equation is rewritten as follows,

$$\log \ln\left\{P(t_0)-P_0/P(t)-P_0\right\}=\alpha \log (t-t_0)+\log \beta\,. \tag{22}$$

The values of α and β were calculated by means of the least square method in all cases and the product moment correlation coefficients computed from all experimental data were practically in the range of 1 and 0.95. The values of τ required until the stress at the stop of deformation become $1/\varepsilon$ were measured on each actual relaxation curve and were found ranging from 48 to 1 950 sec in compression, from 300 to 1 016 sec in tension and from 360 to 2 184 sec in torsion, respectively.

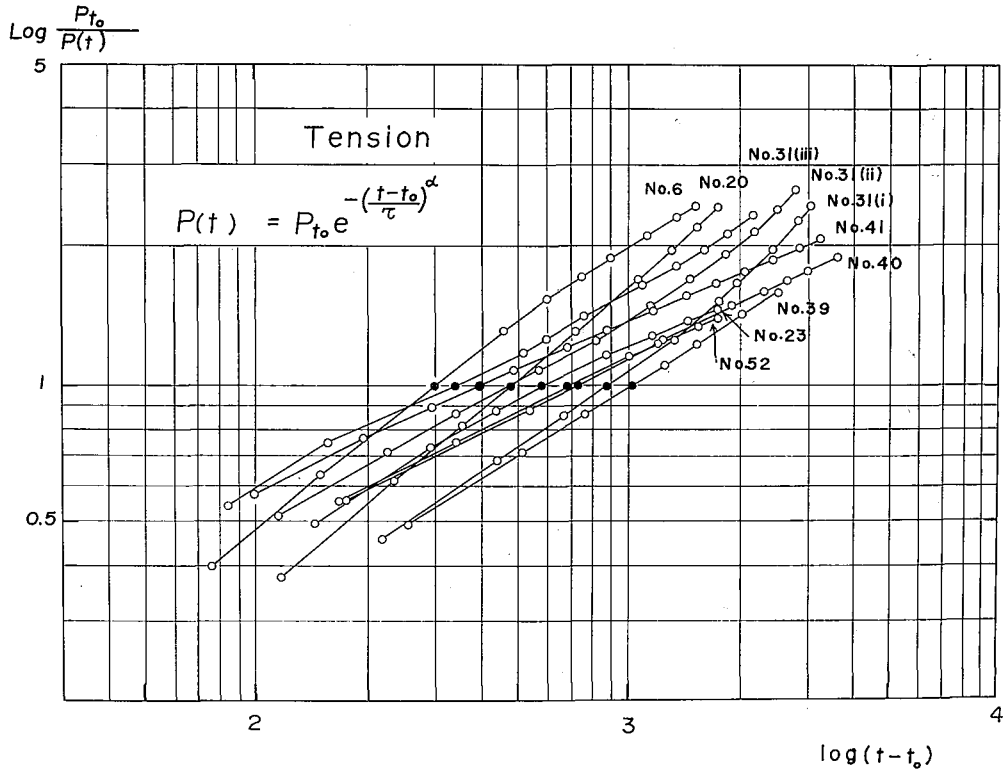

Fig. 18. Examples of an approximate expression on the relaxation curves observed after the tensile deformation of various constant speeds. In this graph, the value of P_0 in eq. (21) is assumed to be zero, according to the tendency of the observed curve.

$t-t_0$: The lapse of time after the time t_0 when the deformation was stopped (in second)

Table 2. The numerical values of the equation approximated or relaxation curves

Compression test					
α :	from	0.247	to	0.694	
τ :	from	0.80	to	32.50	(min)
Tension test					
α :	from	0.348	to	0.673	
τ :	from	5.23	to	16.60	(min)
Torsin test					
α :	from	0.382	to	0.517	
τ :	from	6.10	to	36.40	(min)

Kinosita (1960) obtained 0.5 as the mean value of α in his compression test of constant speed with columnar snow samples and Ôura (1957) obtained 0.443 by analyzing the settling process of the ceiling of a snow cave in horizontally deposited snow. Assuming that, since all values of α are very small, they do not depend on any experimental factors in each test, the above relaxation eq. (21) can be expressed by the mean value

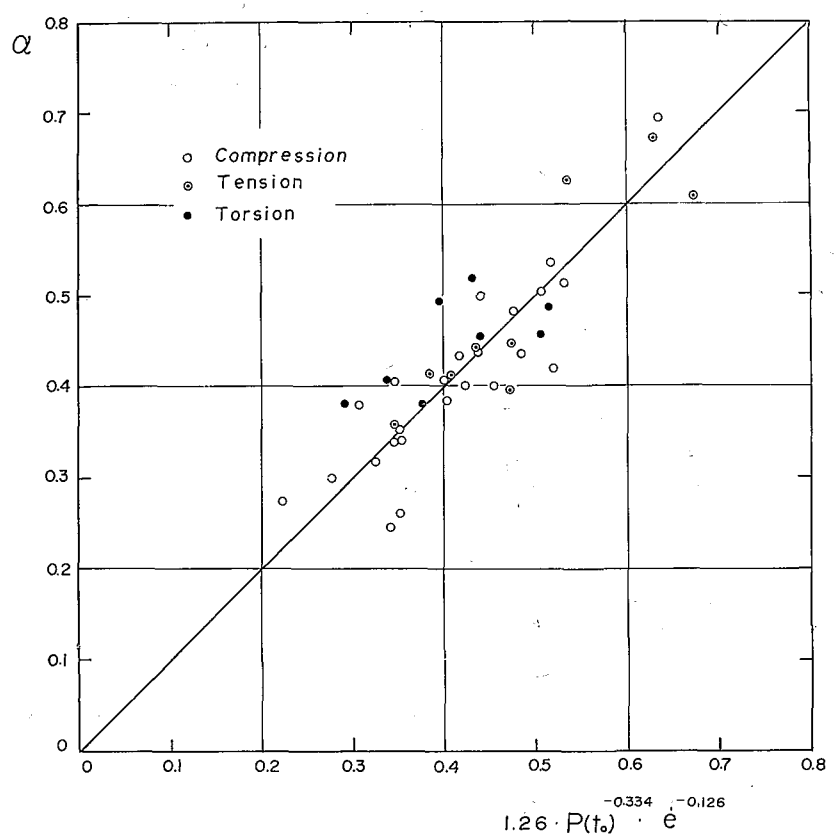

Fig. 19. Dependency of the value α in approximate eq. (21) related to relaxation curves on the experimental factors (the stress at the end of deformation and the strain rate)

from all α as,

$$P(t)=\left\{P(t_0)-P_0\right\}\varepsilon^{-\left(\frac{t-t_0}{\tau}\right)^{0.437}}+P_0\,. \tag{23}$$

Figure 18 shows an expression for the relaxation after the tensile deformation of constant speed. However, a more precise analysis on the values of α and τ shows that they are actually influenced by several experimental factors. Namely,

$$\alpha=1.26\dot{e}^{-0.126}P(t_0)^{-0.334}=1.26\dot{e}^{-\frac{1}{8}}P(t_0)^{-\frac{1}{3}}$$

and

$$\tau=\left(\frac{1}{\beta}\right)^{\frac{1}{\alpha}}=76.5\dot{e}^{-0.856}=76.5\dot{e}^{-\frac{7}{8}}\,. \tag{24}$$

Figure 19 shows the relation between α and the value related to $P(t_0)$ and $\dot{e}$. As seen in this figure, some dispersion of points from the above relation might be influenced by the extent of approximation of an exponential expression for relaxation curves and errors result in which the values of α are computed from that approximate equation by the least square method. In Fig. 20, the relation between the relaxation time τ and the strain rate is shown.

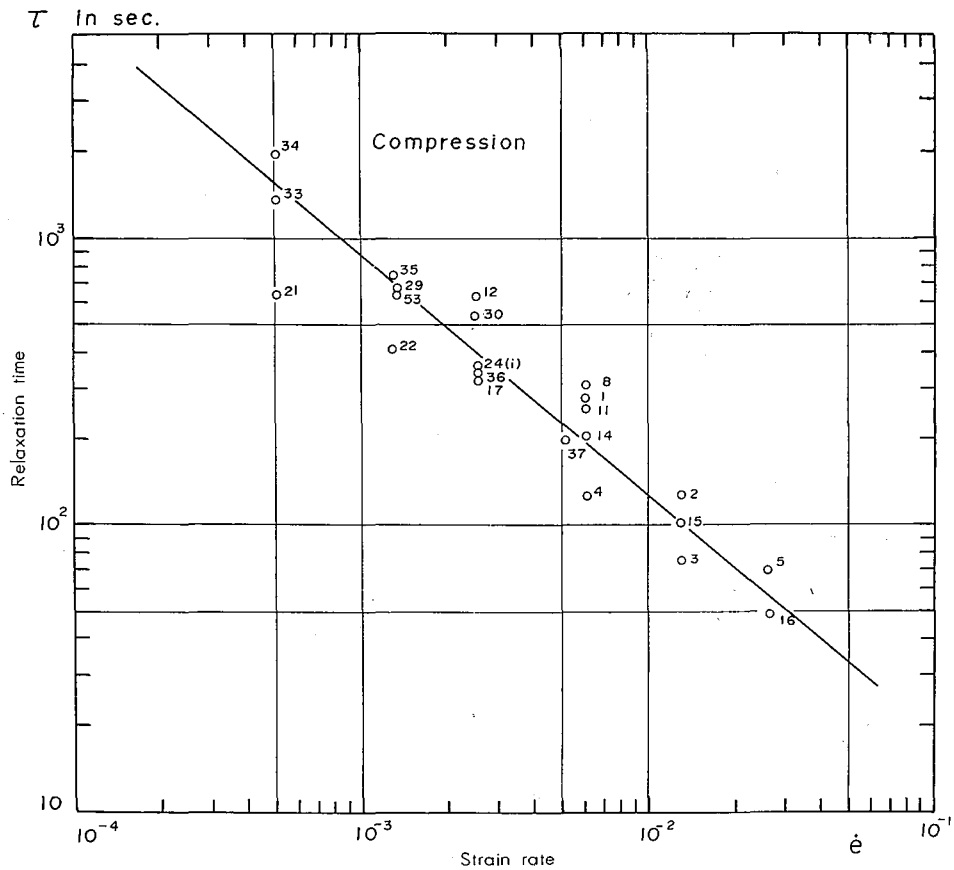

Fig. 20. Dependency of the value τ in the approximate eq. (21) related to the strain rate $\dot{e}$ in relaxation curves

d) *Analysis of stress-time relations on the basis of Boltzmann's fundamental equation*

In general visco-elastic materials, the varying states of stress during the deformation of a constant speed and the relaxation of stress after the stop of that deformation have been generally analyzed on the basis of Boltzmann's fundamental equation expressed as,

$$P(t)=\gamma e(t)-\int_0^t \mathrm{f}(t-t')e(t')\,\mathrm{d}t', \tag{25}$$

where $P(t)$ is the stress at the time t, γ is the coefficient of instantaneous elasticity, which includes the coefficient of static elasticity observed from very steady deformation. In snow, this latter value expressed as γ_0 can be considered as approximately zero at times, because from the results of observation it was shown that the stress stored in the snow sample till the stop of deformation shown as almost complete relaxation after a long time. Therefore, γ is expressed here as γ_1, $\mathrm{f}(t-t')$ is called the after-effect function or memory function, $e(t)$ and $e(t')$ are each strains at the time t and t', respectively.

Stress-time relations were considered by a division into two cases, one of which is the case of $\dot{e}\fallingdotseq$constant throughout deformation and another one is the case of $e(t)=e(t')=e(t_0)=$constant after the end of deformation. This treatment means that the relation of stress will take place continuously in all cases of deformation and therefore the stress actually observed is represented apparently as the difference deduced every time by the stress value relaxing gradually during the deformation from that increasing supposedly in accordance with the initial state of elastic deformation.

Thus Boltzmann's equation is rewritten for the sake of convenience for the following two cases. When the rate of strain $\dot{e}$ is considered as constant, where $0\leq t\leq t_0$, t_0 is the time of the end of deformation.

$$P(t)=\dot{e}\left\{\gamma t-\int_0^t \mathrm{f}(t-t')t'\,\mathrm{d}t'\right\}. \tag{26}$$

Then, when each strain $e(t)$, $e(t')$ are considered as constant after the stop of deformation, where $t_0\leq t$ and the sample length is retained as constant,

$$P(t)=e(t_0)\left\{\gamma-\int_{t_0}^t \mathrm{f}(t-t')\,\mathrm{d}t'\right\}-\dot{e}\int_0^{t_0}\mathrm{f}(t-t')t'\,\mathrm{d}t'. \tag{27}$$

On the other hand, by using the fact that the relation of stress after the stop of deformation can be represented by eq. (21), the expanded coefficient of elasticity $\gamma(t)$ is given in the following expansion. Namely,

$$\gamma(t)=\gamma_0+\gamma_1(t_0)\varepsilon^{-\beta(t-t_0)^{\alpha}}, \tag{28}$$

where $\gamma_1(t_0)$ is the coefficient of elasticity at the stop of deformation, which does not include the coefficient of static elasticity and it is expressed as follows from eq. (27).

$$\gamma_1(t_0)=\gamma_1-\frac{1}{t_0}\int_0^{t_0}\mathrm{f}(t_0-t')t'\,\mathrm{d}t'.$$

Since eq. (21) was experimentally approximated on the relaxation curves obtained after the deformation of various periods t_0, it was assumed for the sake of convenience that this equation would hold in the case of $t_0=0$. Actually, the values of t_0 are ranging from 4.33 to 57.33 (min) corresponding to various strain rates. Accordingly, eq. (28) is

rewritten as follows,

$$\gamma(t)=\gamma_0+\gamma_1\varepsilon^{-\beta t^\alpha}, \tag{29}$$

and $\gamma(t)$ is expressed by definition as,

$$\gamma(t)=\gamma_0+\int_t^\infty \mathrm{f}(x)\,\mathrm{d}x\,; \qquad x=t-t'. \tag{30}$$

Accordingly, from above equation and eq. (29), the after-effect function $\mathrm{f}(t)$ can be calculated as follows.

$$\mathrm{f}(t)=\alpha\beta\gamma_1 t^{\alpha-1}\varepsilon^{-\beta t^\alpha}. \tag{31}$$

To make another attempt for the sake of simplification, the form of the equation taken till the second term of a series-expansion for eq. (21) was adopted for the approximation on relaxation curves. Namely,

$$P(t)=P(t_0)-\Big\{P(t_0)-P_0\Big\}\beta(t-t_0)^\alpha, \tag{32}$$

and by dividing both sides with $e(t_0)$,

$$\gamma(t)=\gamma(t_0)-\gamma_1(t_0)\beta(t-t_0)^\alpha\,; \qquad t_0\le t. \tag{33}$$

Since the above equation holds for any t_0, assuming here that it will hold in the case $t_0\to 0$ as in the case of eq. (28), $\gamma(t)$ can be rewritten as,

$$\gamma(t)=\gamma_0+\gamma_1(1-\beta t^\alpha). \tag{34}$$

From the above equation and eq. (30), $\mathrm{f}(t)$ can be calculated as before,

$$\mathrm{f}(t)=\alpha\beta\gamma_1 t^{\alpha-1}. \tag{35}$$

Therefore, if the value of $\beta(t-t_0)^\alpha$ is obtained as very small, both the after-effect functions will coincide with each other.

Computation of $P(t_0)$

By substituting eqs. (31) and (35) into eq. (26), $P(t)$ can be computed respectively as follows.

According to eq. (31),

$$P(t)=\dot{e}\left\{\gamma_0 t+\frac{\gamma_1}{\alpha\beta^{\frac{1}{\alpha}}}I\left(\frac{1}{\alpha},\ \beta t^\alpha\right)\right\}. \tag{36}$$

This equation $P(t)$ coincides with that shown by Oka and Ôkawa in 1942. The incomplete gamma function I in eq. (36) can be approximated with the following formula.

$$I(\nu,x)\doteqdot\Gamma(\nu)-x^{\nu-1}\varepsilon^{-x}\left\{1+O\left(\frac{1}{x}\right)\right\},$$

where, Γ is gamma function and O is called Landau's symbol.

Accordingly, putting $t=t_0$ and $\beta^{1/\alpha}=1/\tau$ in eq. (36), $P(t_0)$ can be rewritten as,

$$P(t_0)=e(t_0)\left\{\gamma_0+\frac{1}{\alpha}\left(\frac{\tau}{t_0}\right)\Gamma\left(\frac{1}{\alpha}\right)-\frac{1}{\alpha}\left(\frac{\tau}{t_0}\right)^\alpha\varepsilon^{-\left(\frac{t_0}{\tau}\right)^\alpha}\right\}. \tag{37}$$

On the other hand, according to eq. (35), $P(t_0)$ can be obtained in the same manner as before.

$$P(t)=\dot{\varepsilon}\left\{\gamma t-\frac{\beta\gamma_1}{1+\alpha}t^{1+\alpha}\right\}. \tag{38}$$

Putting $t=t_0$ and $\beta^{1/\alpha}=1/\tau$, the above equation can be rewritten as,

$$P(t_0)=e(t_0)\left\{\gamma_0+\gamma_1\left(1-\frac{1}{1+\alpha}\left(\frac{t_0}{\tau}\right)^{\alpha}\right)\right\}. \tag{39}$$

However, the results of the following equation which were obtained by putting $\gamma_1=\gamma_1(t_0)$ in eq. (38) were actually better for the experimental measurements than that computed from eq. (39). Namely,

$$P(t_0)=\frac{\gamma e(t_0)}{1+\dfrac{1}{1+\alpha}\left(\dfrac{t_0}{\tau}\right)^{\alpha}}. \tag{40}$$

Table 3. Examples of the results computed by eq. (40)
Compression test

No.		36	37
$P(t_0)$	g-wt/cm^2	855	1 304
γ	g-wt/cm^2	83.3×10^3	110.0×10^3
$e(t_0)$		2.41×10^{-2}	2.56×10^{-2}
t_0	min	8.83	5.00
τ	min	5.77	3.30
α		0.299	0.277
$P(t_0)$	computed	733	1 359

Consequently, the agreement between $P(t_0)$ computed from eqs. (37) and (39), and $P(t_0)$ measured experimentally were not so good as a rule. This is probably due to having assumed the deformation time t_0 in the approximate equation for relaxation curves as zero when the after-effect function $f(t)$ was obtained.

e) *Consideration of the relaxation curve on the basis of a dynamical model*

Generally the stress relaxation of visco-elastic material can be analyzed theoretically on the basis of the dynamical system consisting of parallel combinations of Maxwell's elements. The relaxation curves are expressed theoretically by the following equation.

$$P(t)=\sum_i P_i\varepsilon^{-\frac{t-t_0}{\tau_i}}\ ;\qquad \tau_i=\eta_i/\gamma_i\,, \tag{41}$$

where $P(t)$ is the stress at the time t, P_i and τ_i are the initial stress and the relaxation time related to the i-th Maxwell's element, γ_i and η_i are the coefficients of elasticity and viscosity, respectively. By dividing this equation with the strain at the end of deformation, the coefficient of elasticity can be expressed as follows, assuming that the distribution of relaxation time is continuous.

$$\gamma(t)=\int_0^{\infty}\Phi(\tau)\,\varepsilon^{-\frac{t-t_0}{\tau}}\,d\tau\,.$$

In order to obtain each value of P_i and τ_i or γ_i and η_i, these distribution functions must be approximated with the several curves of time-differentiation of $\gamma_i\exp[-(t-t_0)/\tau_i]$ for proper τ_i. Accordingly, from eq. (41),

Table 4. The values of the relaxation time, the coefficients of visco-elasticity and the initial stresses related to individual Maxwell's element

Compression No. 29

Density of snow sample ρ: 0.252 g/cm³ (Settled snow)
Test temperature T: −20.5 °C
Compression speed V_c: 0.25 mm/min
Period of deformation t_0: 12.33 min
Total strain $e(t_0)$: 1.65×10^{-2}
Stress at the end of deformation $P(t_0)$: 423 g-wt/cm²

τ_i (min)	P_i (g-wt/cm²)	γ_i (g-wt/cm²)	η_i (g-wt·min/cm²)
0.30	78.28	4.74×10^3	0.142×10^4
3.00	122.03	$7.40\times$ "	$2.22\times$ "
23.33	216.35	$13.11\times$ "	$30.59\times$ "
	$\sum$ 416.66		

Compression No. 30

ρ : 0.251 g/cm³ (Settled snow)
T : −20.5°C
V_c: 0.50 mm/min
t_0 : 4.33 min
$e(t_0)$: 1.09×10^{-2}
$P(t_0)$: 420 g-wt/cm²

τ_i (min)	P_i (g-wt/cm²)	γ_i (g-wt/cm²)	η_i (g-wt·min/cm²)
0.42	92.77	8.51×10^3	0.35×10^4
2.50	152.09	$13.95\times$ "	$3.49\times$ "
18.33	167.29	$15.35\times$ "	$28.14\times$ "
	$\sum$ 412.15		

Compression No. 34

ρ : 0.296 g/cm³ (Settled snow)
T : −23.0°C
V_c: 0.10 mm/min
t_0 : 47.00 min
$e(t_0)$: 2.47×10^{-2}
$P(t_0)$: 759 g-wt/cm²

τ_i (min)	P_i (g-wt/cm²)	γ_i (g-wt/cm²)	η_i (g-wt·min/cm²)
1.33	189.40	7.67×10^3	1.02×10^4
7.50	241.30	$9.77\times$ "	$2.44\times$ "
58.33	320.48	$12.98\times$ "	$75.69\times$ "
	$\sum$ 751.18		

$$-\frac{d\gamma(t)}{d\log(t-t_0)}=\sum_i \gamma_i \ln 10\left(\frac{t-t_0}{\tau_i}\right)\varepsilon^{-\frac{t-t_0}{\tau_i}}. \tag{42}$$

Figures 21 a, b, c are examples of a graph illustrated to obtain the approximate curve by this method. Consequently each curve of $-d\gamma(t)/d\log(t-t_0)$ with respect to

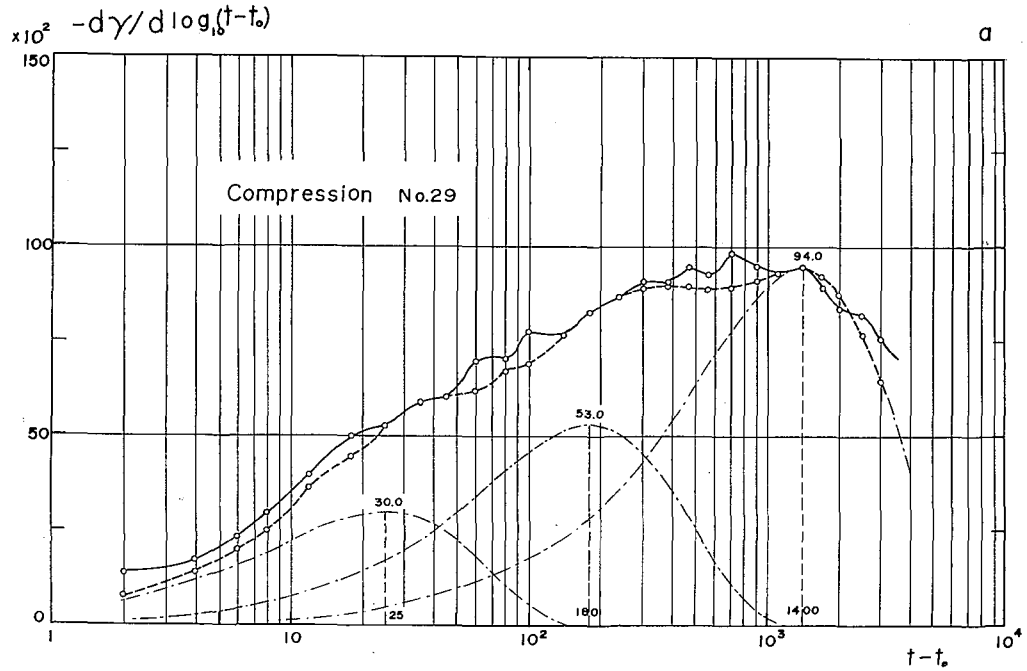

measuring time in seconds

Fig. 21a.

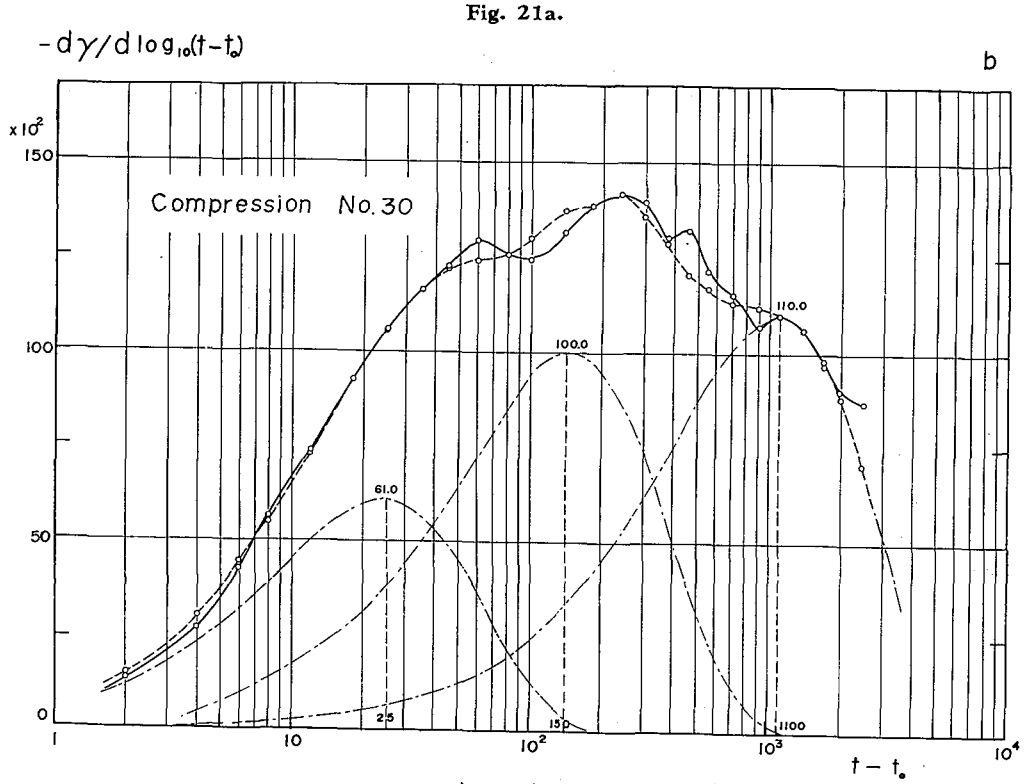

measuring time in seconds

Fig. 21b.

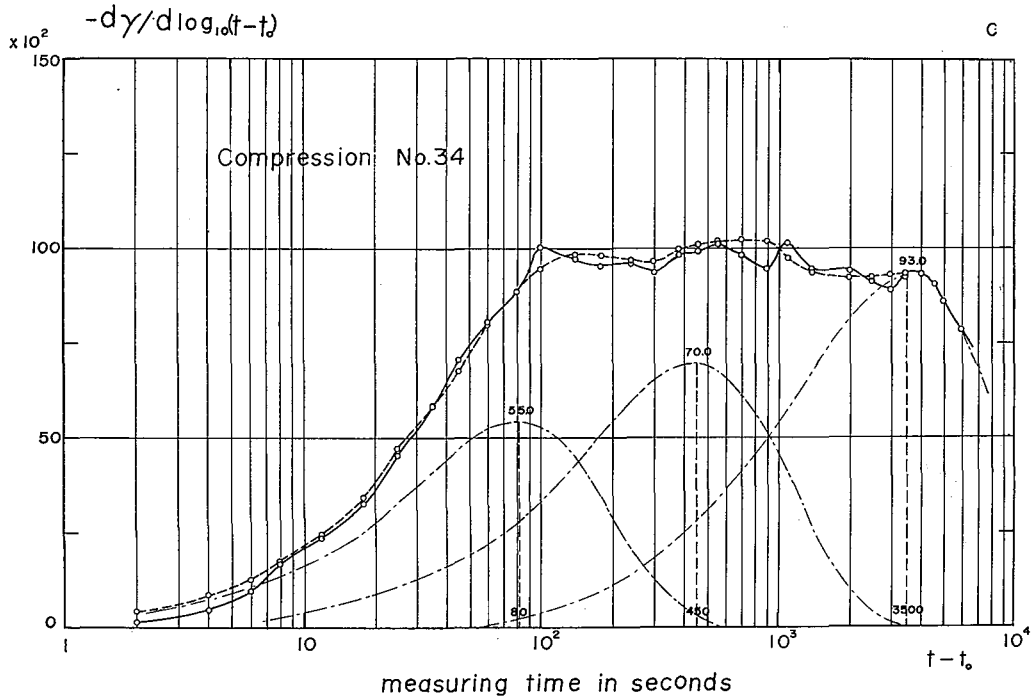

Fig. 21. Curve of $-d\gamma(t)/d\log(t-t_0)$ for test time $(t-t_0)$ in logarithmic scale and approximate curve due to a superposition of three curves obtained from the differentiation of $\gamma(t)$ with test time in logarithmic scale.
$t-t_0$: The lapse of time after the time t_0 when the deformation was stopped

$\log(t-t_0)$ can be subsequently approximated by the superposition of three curves of the time-differentiation of $\gamma_i \varepsilon^{-\frac{t-t_0}{t_i}}$ in logarithmic scale.

Acknowledgments

The author wishes to express his deep appreciation to Profs. Zyungo Yosida and Seiiti Kinosita of the Institute of Low Temperature Science, Hokkaido University in Japan, for their suggestions and in particular, to Dr. Mikio Shoda and my colleagues of the Railway Technical Research Institute in Japan for their constant guidance and valuable advice in the course of these investigations.

Extremely, valuable suggestions were derived from the excellent work of Dr. R. Haefeli who investigated snow mechanics in Switzerland. In the presentation of this manuscript, I am indebted to Prof. Hirobumi Ôura of the Institute of Low Temperature Science, for his instructions of guidance.

References

1) HAEFELI, R. 1939 Schneemechanik mit Hinweisen auf die Erdbaumechanik. *In* Der Schnee und Seine Metamorphose (H. Bader *et al.*, *eds.*), Beitr. zur Geol. der Schweiz, Geotech. Serie Hydrol., Lieferung **3**, Kümmerly u. Frey, Bern, 1-61; through Translation by Jan

C. V. Tienhoven 1954 Snow Mechanics with References to Soil Mechanics. *In* Snow and its metamorphism, *SIPRE Trans.*, **14**, 57–218.

2) KINOSITA, S. 1957 The relation between the deformation velocity of snow and types of its deformation (Plastic and Destructive). *Low Temp. Sci.*, **A 16**, 139–166.*

3) KINOSITA, S. 1958 The relation between the deformation velocity of snow and types of its deformation II. *Low Temp. Sci.*, **A 17**, 11–30.*

4) KINOSITA, S. 1960 The relation between the deformation velocity of snow and the types of its deformation III. *Low Temp. Sci.*, **A 19**, 135–146.*

5) KINOSITA, S. 1962 Transformation of snow into ice by plastic compression. *Low Temp. Sci.*, **A 20**, 131–157.*

6) KINOSITA, S. and WAKAHAMA, G. 1959 Thin sections of deposited snow made by the use of aniline. *Low Temp. Sci.*, **A 18**, 77–96.*

7) KOJIMA, K. 1954 Visco-elastic property of snow. *Low Temp. Sci.*, **A 12**, 1–13.*

8) KOJIMA, K. 1955 Viscous compression of natural snow layer I. *Low Temp. Sci.*, **A 14**, 77–94.*

9) KOJIMA, K. 1956 Viscous compression of natural snow layer II. *Low Temp. Sci.*, **A 15**, 117–136.*

10) KOJIMA, K. 1957 Viscous compression of natural snow layers III. *Low Temp. Sci.*, **A 16**, 167–196.*

11) KOJIMA, K. 1958 Viscous compression of natural snow layers IV. *Low Temp. Sci.*, **A 17**, 53–64.*

12) LANDAUER, J. K. 1955 Stress-strain relation in snow under uniaxial compression. *SIPRE Res. Paper*, **12**, 1–9.

13) ŌURA, H. 1957 On the force with which a beam supports the ceiling of a snow cave. *Low Temp. Sci.*, **A 16**, 55–72.*

14) OKA, S. and ŌKAWA, A. 1942 Recent studies on the mechanical properties of amorphous bodies. *Nihon Sūgaku Buturi Gakkai Si* (*J. Phys.-Math. Soc. Japan*), **16**, No. 3.†

15) SHINOJIMA, K. 1962 Study on the visco-elastic deformation of deposited snow. *Railway Tech. Res. Rept.*, No. **328**, The Railway Tech. Res. Inst., Japanese National Railways, 1–56.†

16) SHODA, M. and SUDŌ, I. 1961 Profile investigation of the snow cover deposited on the horizontal testing court of the snow experiment station, shiozawa during 8 winter periods, 1952–1960. *Railway Tech. Res. Rept.*, No. 258, The Railway Tech. Res. Inst., Japanese National Railways, 1–159.†

17) YOSIDA, Z., SASAYA, M. and UTUMI, T. 1948 Elastic modulus and creeping velocity of snow. *Low Temp. Sci.*, **A 4**, 11–16.*

18) YOSIDA, Z. and Colleagues 1958 Physical studies on deposited snow, IV. Mechanical properties (3). *Contr. Inst. Low Temp. Sci.*, **A 13**, 55–100.

19) YOSIDA, Z. 1965 Rheology of deposited snow. *Oyo Buturi* (*Applied physics*), **34**, 70-79.

* In Japanese with English summary.

† In Japanese.